On rates and styles of late volcanism and rifting on Venus

Alexander T. Basilevsky
Vernadsky Institute of Geochemistry and Analytical Chemistry, Russian Academy of Sciences, Moscow, Russia
Department of Geological Sciences, Brown University, Providence, Rhode Island, USA

James W. Head III
Department of Geological Sciences, Brown University, Providence, Rhode Island, USA

Received 15 February 2001; revised 26 December 2001; accepted 2 January 2002; published 27 June 2002.

[1] We investigated the possibility of significant variations in the rates and styles of volcanism and rifting during the time postdating the formation of regional plains on Venus. We analyzed the age relations of all known impact craters ≥30 km in diameter (183 craters) with the neighboring geologic units. Of these we selected 164 craters which were superposed on regional plains and determined if post-regional-plains (PRP) volcanics and/or PRP rift structures were present in the crater vicinity and if these craters postdated the volcanics and rift structures or predated them. In 53 cases it was possible to determine these relations. On the basis of these relationships, it was found that the general rates of volcanism and rifting during PRP time were close to constant or at least had no drastic changes. This implies a significant change in the rates of volcanism and rifting in the vicinity of the boundary between PRP time and the preceding time, which is marked by the formation of the global wrinkle-ridge network. It was also found that (1) the role of rift-associated volcanism during PRP time was close to constant or slightly decreasing, (2) the role of corona-related volcanism was noticeably decreasing, and (3) the role of noncorona, hot spot volcanism was proportionally increasing. The latter changes may be due to thickening of the lithosphere during PRP time. The results imply also that at most if not all places where PRP rifting occurred, the rift-associated fracturing, when started, continued for a significant part of PRP time. Our conclusions are valid both (1) for the case of a globally synchronous transition from emplacement of regional plains to the PRP regime and (2) for the case of such a transition occurring at different times in different areas of Venus. *INDEX TERMS:* 6295 Planetology: Solar System Objects: Venus; 5475 Planetology: Solid Surface Planets: Tectonics (8149); 5480 Planetology: Solid Surface Planets: Volcanism (8450); 5420 Planetology: Solid Surface Planets: Impact phenomena (includes cratering); 5455 Planetology: Solid Surface Planets: Origin and evolution; *KEYWORDS:* Venus, volcanism, rifting, stratigraphy, geologic history, impact craters

1. Introduction

[2] About 70–75% of the surface of Venus is covered by regional plains which were apparently emplaced as broad-scale basaltic flood deposits [e.g., *Head et al.*, 1992]. The rest of the surface is occupied by volcanic and tectonic features both older and younger than the regional plains [see, e.g., *Barsukov et al.*, 1986; *Head et al.*, 1992; *Price and Suppe*, 1994, 1995; *Crumpler et al.*, 1997]. There is broad agreement among researchers that the end of regional plains formation marks a significant change in volcanic and tectonic rates and styles on Venus although there is considerable debate as to how fast that change was [*Schaber et al.*, 1992; *Phillips et al.*, 1992; *Strom et al.*, 1994; *Namiki and Solomon*, 1994; *Price and Suppe*, 1994, 1995; *Hansen et al.*, 1997; *Crumpler et al.*, 1997; *Tanaka et al.*, 1997; *Guest and Stofan*, 1999; *Basilevsky and Head*, 1998, 2000a; *Head and Basilevsky*, 1998]. We adopt the timescale of *Basilevsky and Head* [1998], *Basilevsky et al.* [1997], *Head and Basilevsky* [1998], and *Basilevsky and Head* [2000a], in which regional plains form the Rusalka Group and are stratigraphically overlain by the Atla Group and the Aurelia Group [see *Basilevsky et al.*, 1997, Figure 9]. The post-regional-plains (PRP) volcanism (also obviously basaltic) is represented mostly by volcanic flows, many of which show association with rifts and coronae, while some do not. Rifting, which was only one of the tectonic processes resurfacing Venus until the end of the regional plains emplacement, becomes in PRP time the only significant tectonic process. There is evidence that the mean rates of volcanism and rifting during PRP time were significantly lower compared to the time of regional plains emplacement [*Basilevsky and Head*, 2000b].

[3] The goal of this work was the more detailed analysis of the post-regional plains (PRP) time (the Atlian and Aurelian periods). We addressed three questions: (1) Was the rate of volcanism during PRP time more or less con-

0148-0227/02/2000JE001471$09.00

stant, generally decreasing, or perhaps increasing after some particular time? (2) Were there noticeable changes with time in the roles of different types of this late volcanism? (3) Was the rate of rifting during PRP time more or less constant, generally decreasing, or perhaps increasing after some particular time? We undertook this assessment through the analysis of impact craters and their age relations with adjacent deposits of PRP volcanics and rift structures. First, we describe the general approach and procedures used in this study. We then describe several typical examples of impact crater age relations with adjacent PRP volcanics and the results of observations on all craters analyzed. Finally, we assess the implications of the observations.

2. Approach and Procedure

[4] In this study we have analyzed the Magellan images of impact craters superposed completely or partly on regional plains. These craters were present when geologic events happened on Venus after the time of formation of regional plains. We analyzed the regions surrounding the craters and assessed the presence of PRP volcanic deposits and rift structures, and in each case they were found we determined if the volcanic deposits and rift-associated structures predated or postdated the specific crater. In general, this approach is close to that used by *Basilevsky et al.* [1999]. Recognizing that large craters and their ejecta occupy larger areas (thus increasing the probability that they will be in contact with PRP volcanics and rifts), we have studied only craters $\geq$30 km in diameter. This size limit is also important in view of potential burial of craters by younger volcanics. Craters $\geq$30 km in diameter have rims standing $\geq$500 m above the precrater surface [*Sharpton*, 1994]. This is larger than the mean thickness of lavas composing large volcanoes ($\sim$360 m, according to *Crumpler et al.* [1997]), which are obviously the thickest among all varieties of PRP volcanics.

[5] The total number of such craters is relatively large, 183 craters of 969 included in the updated version of the *Schaber et al.* [1998] database. We examined all these 183 craters and found that 163 of them are completely or partly superposed on regional plains. For 44 of them we have been able to determine if they are older or younger than the neighboring PRP volcanics, and for 21 craters we have been able to determine the age relations with the neighboring PRP rifts. Some of the craters show age relations with both volcanics and rifts, so the total number of craters showing age relations with volcanics and/or rifts is not 44 + 21 = 65, but only 53.

[6] The 44 craters showing age relations with PRP volcanics represent two different groups (with and without radar-dark parabolas) which will be analyzed separately. We found that 29 of the 44 craters have no associated dark parabola and 15 craters have associated dark parabolas. These 29 craters make up 18% of the total of 160 non-parabola craters $\geq$30 km in diameter found on Venus [*Schaber et al.*, 1998; *Campbell et al.*, 1992]. The 15 dark-parabola craters compose 65% of the total of 23 dark-parabola craters $\geq$30 km in diameter found on Venus. In turn, these 23 craters make up $\sim$13% of 183 craters $\geq$30 km in diameter. The reason why the percentage of craters for which age relations with PRP volcanics have been determined is significantly higher for dark-parabola craters is obvious: Each dark parabola covers an area more than several hundred kilometers across, so the probability that in this large area PRP volcanics are present is rather high. Nonparabola craters may be in contact with PRP volcanics in relation to the crater rims and ejecta blankets, including crater outflows and crater-associated radar dark haloes. So their age relations with PRP volcanics can be determined only if these volcanics are within a relatively small area in close proximity to the crater.

[7] Craters with and without radar-dark parabolas are believed to differ in their age. Dark-parabola craters were probably associated with almost all craters formed on Venus being deposits of crater ejecta settled down through the east-west super-rotating dense atmosphere of this planet [*Campbell et al.*, 1992; *Schultz*, 1992]. But with time these deposits are being reworked by surface processes, so only the most recent craters have the parabolas preserved. Because dark-parabola craters compose $\sim$10% of the crater population of Venus (we ignored small craters which are believed never to have had parabolas), they evidently represent the youngest 10% of the appropriate part of the crater population. This implies that they formed within the latest $\sim$10% of the mean surface age of Venus [*Basilevsky*, 1993; *Strom*, 1993]. If the latter is T, then the mean age of regional plains on Venus is close to T (see discussion by *Basilevsky et al.* [1997, 1999] and by *Basilevsky and Head* [1998, 2000a]), and then the age of the dark-parabola craters is not more than $\sim 0.1T$, while the age of nonparabola craters superposed on regional plains is in the range from T to $0.1T$. In the timescale of *Basilevsky and Head* [1995, 1998, 2000a] the dark-parabola craters belong to the Aurelia Group, while nonparabola craters superposed on regional plains belong to the Atla Group. *Schultz* [1992] has shown that the parabola formation process depends on the direction of impact and on the geographical latitude of the place (through the wind patterns), so some very recent craters may have no parabola. This, however, does not change the conclusion concerning the very recent age of dark-parabola craters.

[8] The number of nonparabola craters (29) seems to be large enough to consider that their formation was more or less evenly distributed along the time axis. If so, then the percentages of craters which are younger or older than the neighboring PRP volcanics should provide information on the general character of the distribution of these volcanics along the time axis (Figure 1). If, for example, a predominant majority of PRP volcanics formed in the beginning of PRP time soon after termination of formation of regional plains (Figure 1a), then most of these 29 craters should show evidence that they postdate the neighboring PRP volcanics. If the predominant majority of PRP volcanics formed very recently (see Figure 1b), one would expect that most of these 29 craters should show evidence that they predate the neighboring PRP volcanics. If formation of PRP volcanics was more or less evenly distributed in time (see Figure 1c), or if formation of PRP volcanics was concentrated in the middle of PRP time (see Figure 1d), then about half of the craters should postdate and about half should predate these deposits. The implications for the cases intermediate between these three are also obvious.

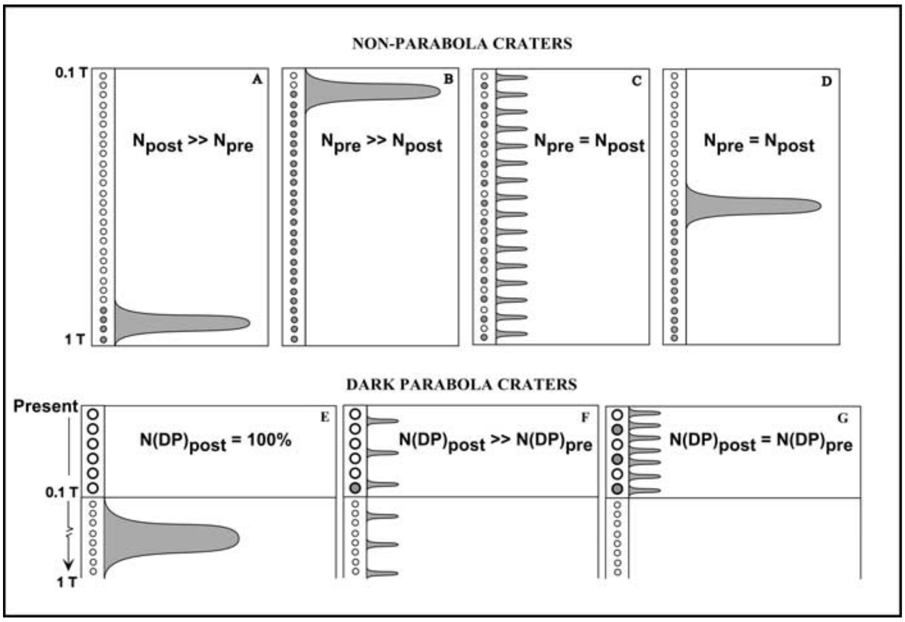

Figure 1. Diagrams showing how the percentages of post-regional plains (PRP) craters postdating and predating the neighboring PRP volcanics provide information on the distribution of the volcanics along the time axis. Vertical columns of circles symbolize the timeline marked by the formation of impact craters. Open circles symbolize craters superposed on PRP volcanics. Solid circles symbolize craters embayed or partly covered by PRP volcanics. (a) PRP volcanics were concentrated in the beginning of the PRP time. Only a small percentage of nonparabola PRP craters have a chance to predate the PRP volcanics. (b) PRP volcanics formed very recently, close to 0.1 *T*. Most of the nonparabola PRP craters have a chance to predate the PRP volcanics. (c) Formation of volcanics was evenly distributed during PRP time. About half of the nonparabola PRP craters have a chance to postdate and about half to predate the PRP volcanics. (d) PRP volcanics are concentrated in the middle of the PRP time. About half of the nonparabola PRP craters have a chance to postdate and about half to predate the PRP volcanics. (e) All PRP volcanics formed before time 0.1*T*. All dark-parabola craters postdate PRP volcanics. (f) PRP volcanics were evenly distributed during the time from *T* until the present. Most of the dark-parabola craters have a chance to postdate and only some of them have a chance to predate PRP volcanics. (g) All PRP volcanics formed during the time from 0.1*T* until the present, and their formation was evenly distributed during this time. About half of the dark-parabola craters have a chance to postdate and about half to predate PRP volcanics.

[9] The number of dark-parabola craters (15) is also probably large enough to consider that they were more or less evenly distributed during the time of their formation, that is, within the period from 0.1*T* until the present. If so, then the percentages of dark-parabola craters which are younger or older than the neighboring PRP volcanics may also be informative in terms of the general character of the distribution of these volcanics along the time axis. If, for example, all PRP volcanics on Venus formed before time 0.1*T* (Figure 1e), all these 15 craters should show evidence that they postdate the neighboring PRP plains. If the rate of formation of PRP volcanics on Venus was rather constant throughout the time period from *T* until the present (see Figure 1f), the percentage of craters predating the neighboring PRP volcanics should be an order of magnitude smaller than the percentage of craters postdating these volcanics. If we know from other data the general character of the rate of formation of PRP volcanics, then the observed percentages of dark-parabola craters predating and postdating the volcanics puts constraints on the age of dark-parabola craters. If all PRP volcanics on Venus formed within the time period from 0.1*T* until the present (see Figure 1g), and their formation was more or less evenly distributed along the time axis, then about half of these 15 craters should show evidence that they postdate the neighboring PRP volcanics, while another half should show that they predate these volcanics.

[10] The number of craters showing relations with PRP rifts is 21. Among them, 16 (76%) have no dark parabolas, and 5 (24%) are craters with dark parabolas. The latter percentage is significantly higher than might be expected both from the percentage of dark-parabola craters among those $\geq$30 km in diameter (13%) and from the percentage accepted for relatively large craters in general (10%) [*Campbell et al.*, 1992; *Basilevsky*, 1993; *Strom*, 1993]. Unlike the situation with the analysis of crater/volcanics age relations, the parabolas were not used for determining age relations of these craters with rifts because they efficiently darken the plains but do not tend to darken rough surfaces including rift-associated structures. For dark-parabola craters we determined age relations with rifts in a manner similar to the case of nonparabola craters through analysis of crosscutting/superposition relations between the craters (floor, rim, ejecta) and rifts. So in this analysis of age

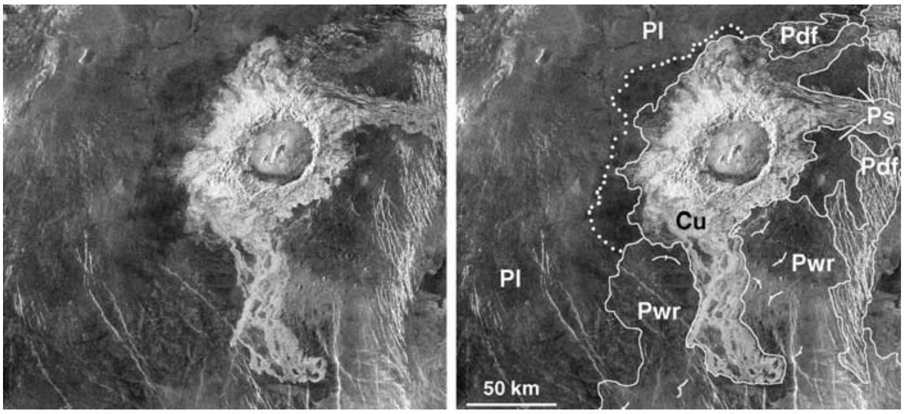

Figure 2. Crater Volkova and its deposits (Cu) superposed on regional plains (Pwr), remnants of Densely fractured plains (Pdf) and on PRP volcanics (Pl, Ps). The dotted line shows the approximate boundary of the crater-related surface darkening. Hereinafter, lines with single hatch show the position of some wrinkle ridges. Portion of C1 MIDRP 75N254;1.

relations with rifts, we do not see any reason for an observational bias between the dark-parabola and nonparabola crater subpopulations. We also do not see any geological reason for the large percentage of dark-parabola craters (we observe 5 dark-parabola craters instead of the 2 or 3 expected) and believe that it is a stochastic variation. But, in any case, because nonparabola and dark-parabola craters represent two parts of the crater population that differ in age, we consider separately these two varieties of craters showing age relations with rifts. The logic of the interpretation of the observed percentages of craters postdating and predating rifts is the same as in the case with volcanics.

[11] In the photogeological study of the craters and their vicinities we used Magellan images (C1MIDRPs, FMIDRPs, and FMAPs), mostly in digital format. For practically all cases where age relations with PRP volcanics could be determined, we made photogeologic maps. In the mapping and description of these areas we used geologic units suggested by *Basilevsky et al.* [1997] and *Basilevsky and Head* [1998, 2000a]. What is called here and by other workers "regional plains" are our units Plains with wrinkle ridges (Pwr) and the majority of Shield plains (Psh). We consider emplacement of the wrinkle ridges deforming these units as the episode separating the time of regional plains formation from post-regional-plains (PRP) time. In the timescale of *Basilevsky and Head* [1995, 1998, 2000a] the emplacement of the wrinkle-ridge network separates the Rusalkian materials from the Atlian and Aurelian ones. The PRP volcanics are not deformed by wrinkle ridges. In the stratigraphic model of *Basilevsky and Head* [1998, 2000a] they are represented by Lobate plains (Pl) and by part of Smooth plains (Ps) which belong to the Atlian and Aurelian Groups. Another part of Smooth plains of *Basilevsky and Head* [1998, 2000a], which resulted from impact-crater-related and eolian activity, has not been mapped in the current study. We used as a guide for this study and as a source of the crater names and sizes the updated version of *Schaber et al.*'s [1998] crater database available at http://wwwflag.wr.usgs.gov/USGSFlag/Space/venus. Names of other surface features were taken from the U.S. Geological Survey planetary nomenclature site: http://wwwflag.wr.usgs.gov/USGSFlag/Space/nomen/vgrid.html.

3. Typical Examples of Age Relations of Craters With PRP Volcanics and Rifts

[12] Here we first describe seven examples of craters superposed on regional plains and showing age relations with neighboring PRP volcanics: five nonparabola craters (two postdating and three predating the volcanics) and two dark-parabola craters (one postdating the volcanics and one which is postdating some of the PRP volcanics in its vicinity and predating others). Then we will describe three craters superposed on regional plains and showing age relations with neighboring PRP rifts: one postdating the rift, one predating the rift, and one postdating some of the rift structures and predating others (Figure 1).

3.1. Crater Volkova

[13] This crater (75.16°N, 242.17°E, D = 47.5 km) is superposed on the eastern apron of lava flows of Renpet Mons volcano at the very north part of Kawelu Planitia. The lava flows are represented by geologic units of Lobate plains (Pl) and Smooth plains (Ps) (Figure 2). They clearly overlap regional plains whose surface is deformed by wrinkle ridges (unit Pwr). Kipukas of a highly fractured unit probably similar to Densely fractured plains (Pdf) of *Basilevsky and Head* [1995, 1998, 2000a] are seen in the western part of the area described. Crater Volkova has both blocky ejecta, composing the majority of its rim, and crater outflow deposits. Blocky ejecta deposits are in contact with Pwr, Pl, and Ps units. The distal ends of the blocky ejecta blanket typically show a gradual transition to the plains units: radar-bright blocky ejecta changes into areas where the darker plains surface is seen among separate blocks, and farther outside, separate blocks are seen among the plains. In some places, however, the ejecta-plains contact looks rather sharp.

[14] Crater outflow deposits, as in the case of other craters on Venus [*Schaber et al.*, 1992], originate within the blocky deposits. In the case of crater Volkova they

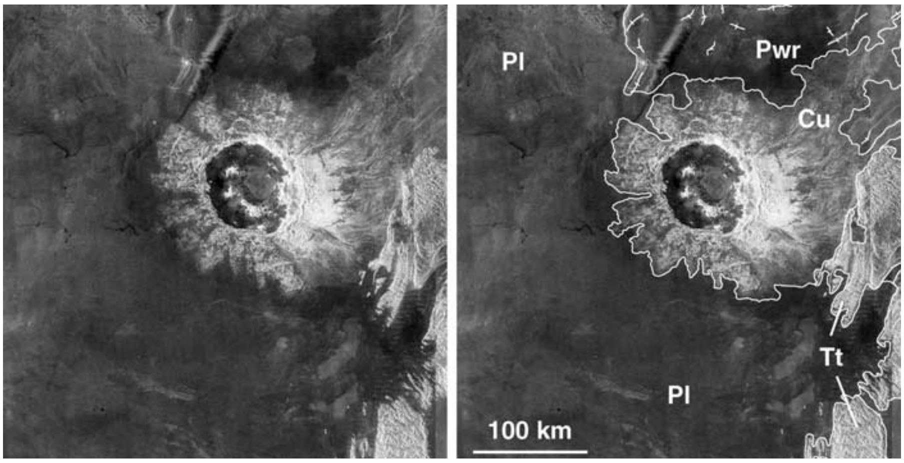

Figure 3. Crater Potanina and its deposits (Cu) superposed on regional plains (Pwr), remnants of Tessera terrain (Tt), and on PRP volcanics (Pl). Portion of C1 MIDRP 30N045;1.

extend outside to the NE, east, and south, forming textured flows. The outflows here are obviously superposed on Pwr and Ps units and locally embay the kipukas of Pdf. Plains units in the close vicinity of the crater look darker than at some distance away. This phenomenon of dark margins or dark haloes was earlier described for Venus craters by *Schaber et al.* [1992]. They are probably due to the presence of rather fine debris produced by the cratering event. Locally on the surface of the Pl unit are seen radar-dark sinuous features a few kilometers wide and 20–30 km long. These are so-called wispy streaks described by *Greeley et al.* [1992] as eolian features whose presence here is probably related to the presence of fine debris produced by the crater formation. In summary, the crater Volkova shows evidence of its superposition on both regional plains (here Pwr) and on PRP volcanics (here Pl and Ps): (1) the gradual termination of blocky ejecta, (2) obvious superposition by the crater outflows, and (3) darkening of the close vicinity of the crater (Figure 1).

3.2. Crater Potanina

[15] This crater (31.62°N, 53.09°E, D = 94.2 km) is superposed on the eastern apron of lava flows from Nix Mons volcano, which is within the Bell Regio topographic rise. Flows of this volcano are represented here by unit Pl, which is superposed on regional plains (unit Pwr) in the north of the described area and embays a few kipukas of Tessera terrain material (Tt) in the south (Figure 3). Crater Potanina has blocky ejecta and an outflow deposit. Pl and Pwr units close to the crater are strongly darkened. At some distance from the crater, where these plains units are not so dark, they have wispy streaks on their surfaces. Contacts of the crater blocky ejecta with Pl and Pwr plains are locally gradual, similar to that described for the ejecta of crater Volkova, but in places, where the crater dark margins are the most prominent, the ejecta terminations look rather sharp. This phenomenon also was described earlier by *Schaber et al.* [1992]. The crater outflow deposit originates in the eastern part of the blocky ejecta blanket and forms the prominent flow going NE, covering Pwr and embaying Tt units. In summary, the crater Potanina shows evidence of its superposition both on regional plains (here Pwr) and on PRP volcanics (here Pl) (Figure 1). In contact with Pwr and Pl it shows (1) gradual termination of blocky ejecta (locally) and (2) prominent darkening of the plains in close proximity to the crater. The crater also shows (3) obvious superposition of its outflow deposits on Pwr.

3.3. Crater Gautier

[16] This crater (26.34°N, 42.82°E, D = 59.3 km) is at the south end of the lava apron of Tepev Mons volcano, sitting within the Bell Regio topographic rise. Lavas of this volcano (Pl) are superposed on the regional plains (Pwr), and they have heavily flooded the crater Gautier, leaving unburied most of the southern part of its rim and the adjacent blanket of blocky ejecta (Figure 4). The crater ejecta is clearly superposed on a small remnant of Pwr among the Pl. It is well seen that the ejecta blanket covers wrinkle ridges completely or partially, depending on their heights. The termination of crater ejecta at the contact with Pwr appears gradual, similar to that described for the crater Volkova. At this termination some darkening of the Pwr surface is observed; however, its scale and prominence are much lower compared to the cases of craters Volkova and Potanina. The boundaries of the crater rim and ejecta with Pl lavas are very sharp and distinct although both these units are radar bright. In some cases it is possible to see how lavas separate crater material into isolated outcrops. The lava surface shows no change in its brightness at the contacts with crater materials. So the crater Gautier shows clear superposition on Pwr regional plains (gradual termination of the distal ends of ejecta, burial of wrinkle ridges) and also clear flooding by Pl lavas (obvious flooding of the crater morphologic elements, sharp contacts between the Pl lavas and crater materials) (Figure 1).

3.4. Crater Kenny

[17] This crater (44.35°S, 271.05°E, D = 52.7 km) is at the NW foot of Abeona Mons volcano in the SW part of Themis Regio. Lavas of this volcano (unit Pl) are superposed both on the regional plains (Pwr) and on the crater (Figure 5). To the north and west of the crater there are

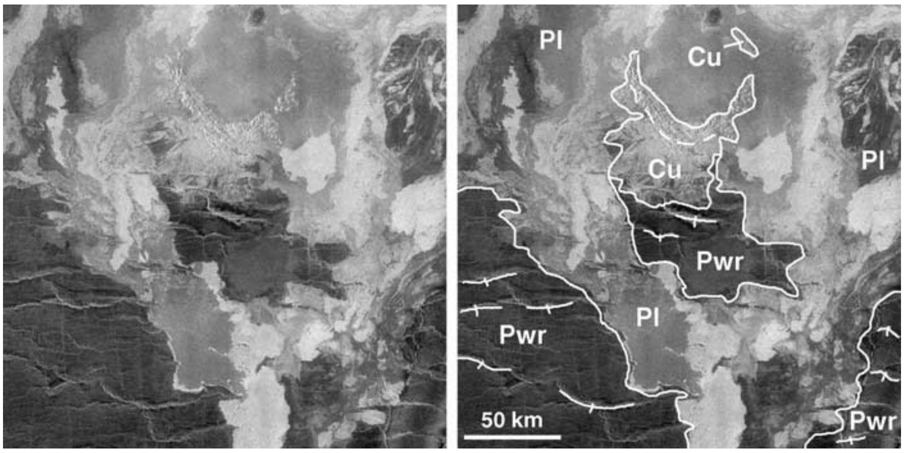

Figure 4. Crater Gautier and its deposits (Cu) superposed on regional plains (Pwr) and heavily flooded by PRP volcanics (Pl). Portion of C1 MIDRP 30N045;1.

kipukas of Tessera terrain (Tt). All units in the northern part of the area considered (including Pl) are significantly darkened by the parabola of crater Sabin, which is ~700 km to the NW. Crater Kenny has a blanket of blocky ejecta and two outflows. The blocky ejecta at the NW sector of the crater is superposed on Pwr plains. The character of the contact is significantly obscured by the parabola-related darkening. The blocky ejecta deposits south and east of the crater are flooded and embayed by the Pl lavas. The contact looks sharp. The eastern part of the crater rim is almost completely flooded by Pl lavas. Adjacent to this part of the rim, on the crater floor, is observed a flow-like feature appearing similar to some nearby Pl flows and probably related to the Pl flow. The crater outflow deposits are observed to the north and to the east of the crater, being clearly superposed on Pwr. Details of their structure are significantly obscured by the Sabin parabola. In summary, crater Kenny postdates Pwr regional plains (most evident from superposition by crater outflows) and predates emplacement of Pl lavas of Abeona Mons volcano (flooding of crater morphological elements by Pl lavas, sharp contact between the lavas and crater materials) (Figure 1).

3.5. Crater Fossey

[18] This crater (2.02°N, 188.72°E, D = 30.4 km) is in the eastern part of Rusalka Planitia, mostly composed here of Pwr plains with relatively small kipukas of ridged and fractured material similar to Ridged and fractured plains (Pfr) of *Basilevsky and Head* [1995, 1998, 2000a]. Maat Mons volcano is located to the east of the crater. The crater clearly postdates Pwr regional plains: crater blocky ejecta has gradual terminations at its contacts with Pwr, crater outflow deposits are obviously superposed on Pwr plains to the north, and the surface of Pwr plains in the close vicinity of the crater is significantly darkened (Figure 6). About 60 km east and SE of the crater, one of the flows of Maat Mons volcano (Pl) is seen overlying the Pwr unit and approaching the crater from the SE. This Pl flow is radar bright both at a far distance from the crater and close to the crater in the

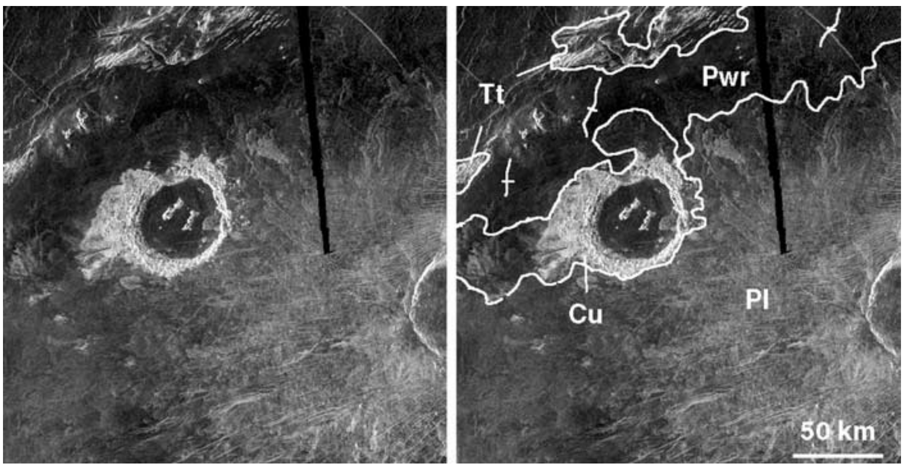

Figure 5. Crater Kenny and its deposits (Cu) superposed on regional plains (Pwr) which embay remnants of Tessera terrain (Tt). Crater is flooded by PRP volcanics (Pl). Portion of C1 MIDRP 45S265;1.

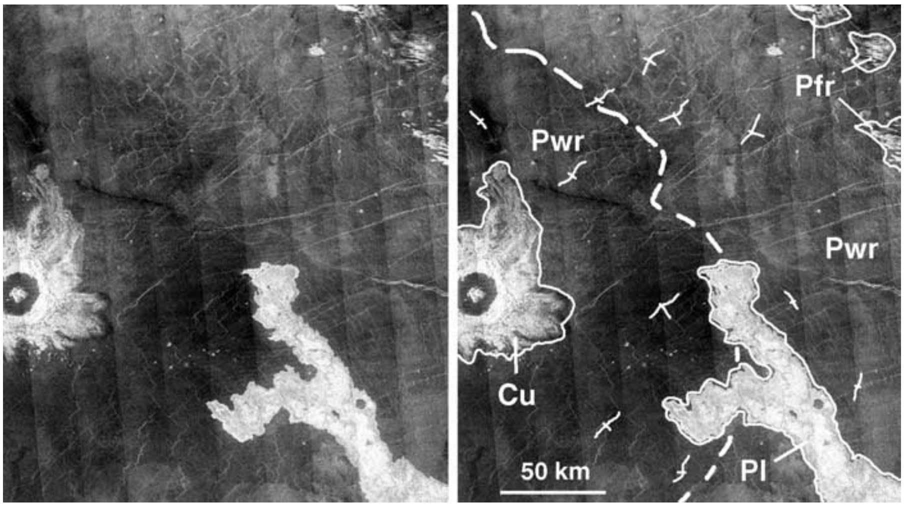

Figure 6. Crater Fossey and its deposits (Cu) superposed on regional plains (Pwr) which embay remnants of Plains with ridges and fractures (Pfr). The crater is surrounded by the area of surface darkening (dashed line). The darkening influences Pwr plains and does not influence the PRP volcanics (Pl). Portion of C1 MIDRP 00N180;1.

area, where the Pwr surface adjacent to this flow is significantly darkened. This probably means that this Pl flow was emplaced here after the formation of the crater Fossey; otherwise, in the close proximity of the crater it would be darkened in a manner similar to the way that the neighboring Pwr plains are (Figure 1).

3.6. Crater Boulanger

[19] This dark parabola crater (26.63°S, 99.25°E, *D* = 71.5 km) is within Tahmina Planitia north of Juno Chasma. It is superposed on a relatively small massif of Tessera terrain (Tt) and on the neighboring regional plains (Pwr) (Figure 7). The crater has blocky ejecta, mostly superposed on Tt to the east, and outflow deposits, mostly superposed on Pwr to the west. The prominent dark parabola associated with this crater extends hundreds of kilometers to the NW and SE, darkening the units which are there. To the SE of the crater the parabola darkens part of the field of Lobate lava flows (Pl) emanating at the contact with densely fractured terrain of Gefjun Corona (Pdf), which sits within the Juno Chasma rift zone. At least part of that rift is rather old, being represented by fragments of Fracture Belt terrain (FB). Darkening of the Pl flows by the parabola material is unambiguous evidence that formation of crater Boulanger postdated the emplacement of these Pl flows (Figure 1).

3.7. Crater Uvaysi

[20] This dark-parabola crater (2.34°N, 198.25°E, *D* = 38.9 km) is in Atla Regio in the area between two giant volcanoes: Ozza Mons to the east and Maat Mons to the

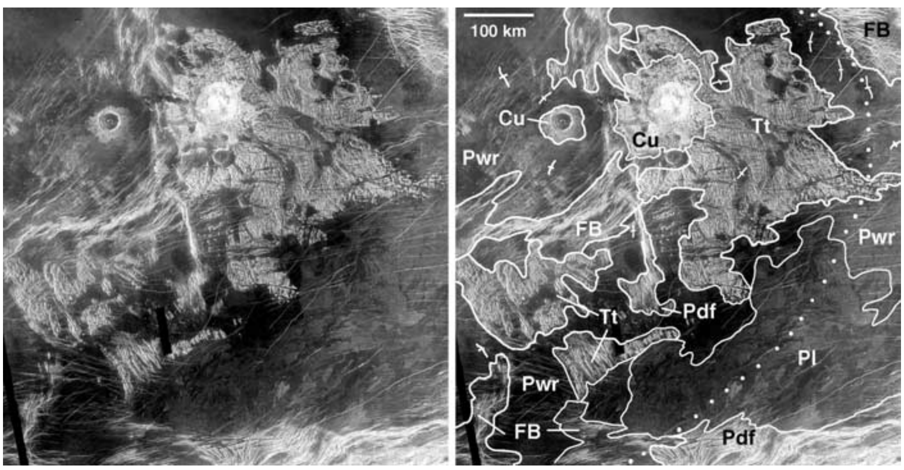

Figure 7. Dark-parabola crater Boulanger and its deposits (Cu) superposed on regional plains (Pwr) and on tessera terrain (Tt). Densely fractured plains (Pdf) and Fracture belts (FB) are also present in the area. About 100 km to the west is crater Simonenko (also Cu). Radar-dark parabola associated with Boulanger (dotted line) darkens both regional plains (Pwr) and PRP volcanics (Pl). Portion of C1 MIDRP 30S099;1.

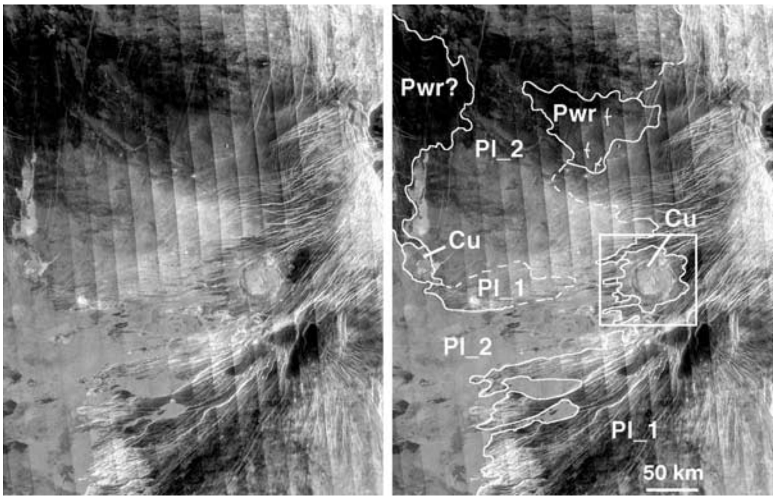

Figure 8. Dark-parabola crater Uvaysi and its deposits (Cu) superposed on PRP volcanics (Pl_1, Pl_2). The dark parabola associated with crater Uvaysi darkens some Pl plains and regional Pwr plains. The white box shows the position of Figure 9. Portion of C1 MIDRP 00N197;1.

west. The first one sits at the junction of several rifts. The second one shows no visible association with rifts. The dark parabola of this crater covers lavas of these two volcanoes and Pwr regional plains (Figure 8). In the vicinity of the crater, lavas of Ozza Mons (Pl_1) are deformed by the NE trending fractures associated with the rift system on which this volcano sits, while lavas of Maat Mons (Pl_2) are not fractured here and clearly cover Pl_1 (Figure 9). Crater Uvaysi postdates Pl_1 lavas (its ejecta is obviously superposed on them, covering not only the lava material but also fractures in it). Pl_2 lavas in the form of tongue-like flows enter the western part of the crater ejecta and cover it. On the crater floor a NE trending narrow fracture and an associated radar-bright flow-like feature are seen. This is probably a late rift fracture which served as a conduit for this flow of Pl_2 lava (possibly a dike-related fracture). In summary, the crater Uvaysi shows evidence that it postdates lavas of Ozza Mons volcano and predates lavas coming from Maat Mons volcano (Figure 1). Because crater Uvaysi belongs to the category of dark-parabola craters, this means that these Maat lavas are very young [*Basilevsky*, 1993; *Strom*, 1993].

3.8. Crater Sitwell

[21] This is a dark-parabola crater (16.64°N, 190.40°E, $D = 32.8$ km) superposed on the Ganis Chasma rift north of Atla Regio. The rift here cuts Pwr plains and relatively small outcrops of older Tessera terrain (Tt) and Fractured and ridged plains (Pfr) (Figure 10). The rift (RT) here has a WNW trending trough ~50 km north of the crater. The trough is ~100 km wide. Its floor, walls, and southern and northern flanks (each ~100 km wide) are cut by numerous graben and faults trending generally E-W, NW, and ENE. Crater Sitwell is superposed on the southern flank of the rift

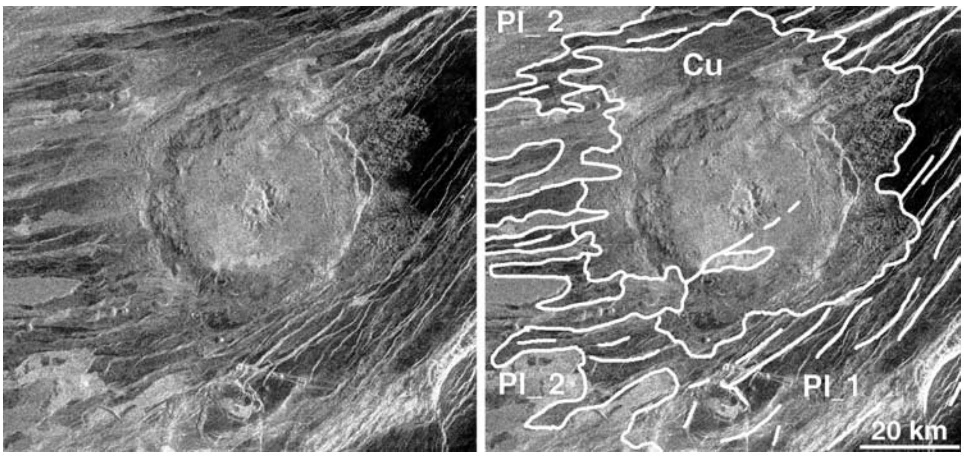

Figure 9. Crater Uvaysi and it deposits (Cu) superposed on PRP lavas of Ozza Mons (Pl_1) and rift-associated fractures (solid lines). Crater deposits are locally covered by lavas of Maat Mons (Pl_2). On the crater floor are seen small Pl_2 lava flows and faint rift-associated fractures (dashed line). Mosaic of parts of *F* MIDRP 00N194;1 and *F* MIDRP 05N194;1.

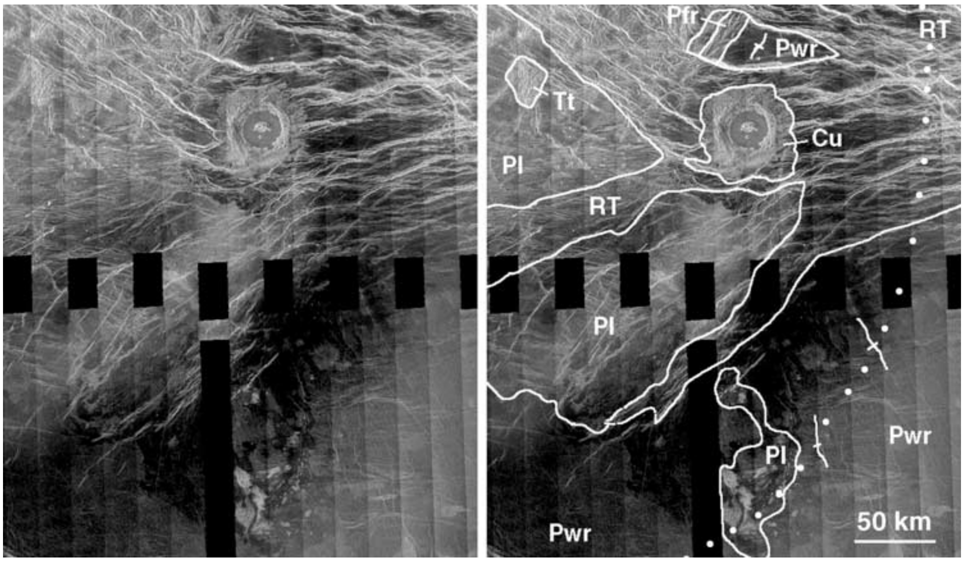

Figure 10. Crater Sitwell and it deposits (Cu) superposed on PRP rift (RT) which cuts regional plains (Pwr) and remnants of Plains with ridges and fractures (Pfr) and Tessera terrain (Tt). Crater-associated parabola (dotted line) darkens regional plains and PRP flows (Pl). Portion of C1 MIDRP 15N197;1.

zone. Its ejecta covers numerous fractures and graben. There is no evidence of fracturing of the crater floor, rim, and ejecta. The associated dark parabola darkens effectively only the plains areas. The rift fractures and graben show no significant darkening. This is evidently due to the effective backscatter on the structure slopes where mirroring facets of rock fragments supposedly covering the structure slopes do not hold the parabola-forming material.

3.9. Crater Balch

[22] This crater (29.90°N, 282.91°E, D = 40 km) is in the Devana Chasma rift within Beta Regio at the southern foot of Rhea Mons. Here Pwr plains and relatively small massifs of tessera (Tt) are cut by graben and faults of the rift (RT) (Figure 11). Crater Balch is superposed on Pwr plains. Within parts of the plains not damaged by rifting, the crater ejecta show a gradual termination. The crater is heavily deformed by rift structures. The rift deformation shifted the eastern part of the crater by ~10 km to the east (first noted in early analysis of the Magellan data by *Solomon et al.* [1992]). There is no evidence of rift-associated structures predating the crater. No radar-dark halo is seen in association with crater Balch.

3.10. Crater Batten

[23] This crater (15.2°N, 217.4°E, D = 65 km) is within the fractured area which is a branch of the rift zone of Ulfrun Regio. The crater is superposed on Pwr plains and on the rift-associated Pl volcanics to the NE of the crater (Figure 12). These two units are superposed by the crater outflows. Pwr plains are deformed by numerous rift-associated fractures, while Pl volcanics are deformed by only a few of them. Crater ejecta obviously covers some of the rift fractures. Other fractures also obviously cut the ejecta and the crater floor. North of the crater there is a field of volcanic shields (Psh2). They are typically 3–5 km in diameter and seem to show no deformation by wrinkle ridges. The age relation between the crater and the Psh2 field is not clear.

3.11. Summary of the Examples

[24] The above descriptions provide the possibility of formulating evidence of craters both postdating and predating the neighboring volcanics (and other units as well) (Figure 1). The age relations between craters and rift-associated structures are rather obvious and do not require special discussion of the evidence for postdating and predating relationships. For crater-volcanics relations we designate the pieces of evidence by numbers which are used in Tables 1 and 2, listing all the craters for which we have found evidence of examples postdating or predating the neighboring pre-regional-plains volcanics. The lines of evidence are as follows:

1. Observations show that ejecta of craters superposed on the unit typically have gradual terminations at the distal ends of the ejecta.
2. Superposition of crater outflow deposits (if they are present at the particular location) on neighboring units is usually very obvious and represents reliable evidence of crater superposition.
3. Darkening of the neighboring units by crater-related dark haloes represents evidence of postdating surrounding units.
4. Darkening of the neighboring units by crater-related parabolas represents evidence of postdating surrounding units. Unfortunately, in some cases there is more then one crater at the location, and then it may be difficult to judge which of the craters is a source of the darkening.
5. Flooding or embayment of craters by younger volcanics typically leads to sharp contacts of crater ejecta with the lavas.
6. In some cases, flooding and embayment are very extensive and obviously destroy key elements of crater morphology.

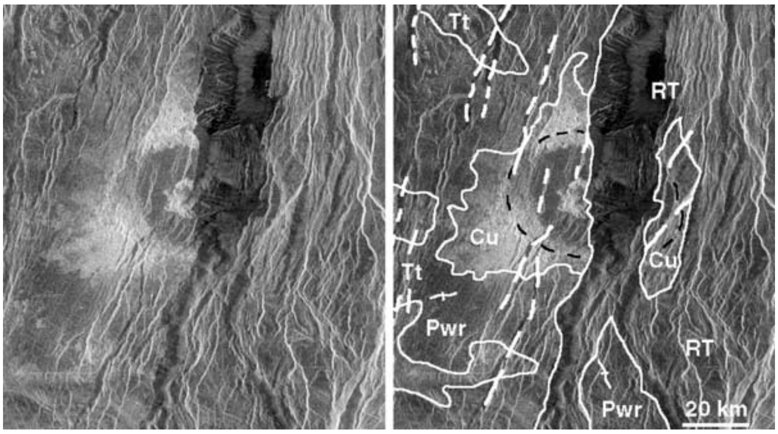

Figure 11. Crater Balch and it deposits (Cu) cut by PRP rift (RT) which also cuts regional plains (Pwr) and remnants of Tessera terrain (Tt). Portion of C1 MIDRP 30N279;1.

7. The absence of darkening of young lava flows by the crater-related halo while neighboring older units are darkened is one more line of evidence that the crater predates emplacement of this lava.

4. Observational Results and Primary Interpretations

[25] As discussed in section 2 (Figure 1), we have studied images of 183 impact craters $\geq$30 km in diameter listed in the *Schaber et al.* [1998] database and found that 163 of them are completely or partly superposed on regional plains deformed by wrinkle ridges. For 53 of 163 craters it was possible to determine if they are older or younger or both older and younger than the neighboring post-regional-plains (PRP) volcanics and rifts. The results of this analysis are summarized for crater-volcanics relations in Table 1 (29 craters having no dark parabola) and Table 2 (15 dark-parabola craters) and are shown in Figure 13. For crater-rift relations the results are summarized in Table 3 (16 nonparabola craters) and Table 4 (5 dark-parabola craters) and are shown in Figure 14. Among these 16 + 5 = 21 craters, there are 12 craters which also show age relations with PRP volcanics and thus are listed in Tables 1 or 2 and 9 craters which show age relations only with rifts.

[26] As follows from Table 1, among 29 craters having no dark parabola, 18 craters (62%) show evidence of postdating the neighboring PRP volcanics and 11 craters (38%) show evidence of predating these volcanics. Of 18 cases when craters postdate the PRP volcanics, 3 cases are questionable. Of 11 cases when craters predate the PRP volcanics, 2 cases are questionable. Even if we were to change the interpretation of the questionable cases into the opposite one (pre instead of post and vice versa), the situation would be the same: the minor predominance of cases post over cases pre. It is possible that some craters, which would be pre, are completely buried by PRP volcanics, which would make a bias in favor of craters post. However, as it was mentioned in section 2, the dominant majority of PRP lavas have a thickness significantly less than the rim heights of the craters under study. The crater

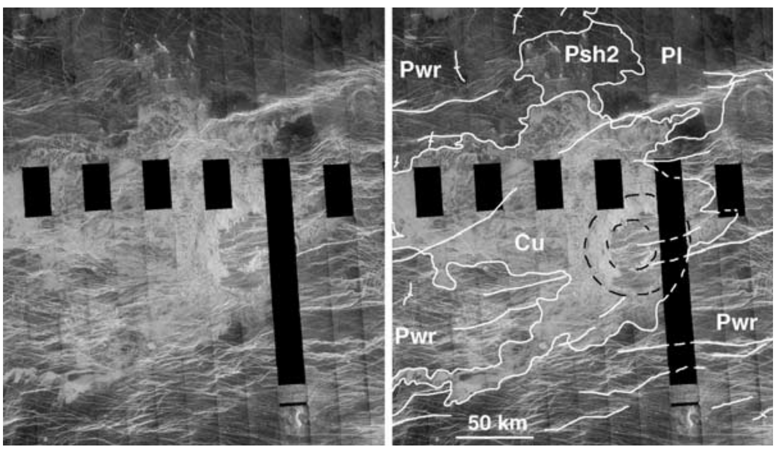

Figure 12. Crater Batten and it deposits (Cu) superposed on regional plains (Pwr). The plains are cut by numerous rift-associated fractures. Some of the fractures are covered by the crater deposits, while others cut the crater and its deposits. Portion of C1 MIDRP 15N215;1.

Table 1. Nonparabola Craters ≥30 km in Diameter Superposed on Regional Plains and Showing Age Relations With Neighboring Post-Regional-Plains Volcanics

	Name	Latitude, deg	Longitude, deg	Diameter, km	Relation to PRPV	Evidence[a]	Source of PRPV
1	Volkova	75.16	242.17	47.5	post	1, 3	Renpet Mons
2	Lonsdale	55.60	222.35	43	pre	6	Marake Colles
3	Potanina	31.62	53.09	94.2	post	1, 3	Nix Mons
4	Gautier	26.34	42.82	59.3	pre	6	Tepev Mons
5	O'Keeffe	24.51	228.78	76.9	post ?	2	Pani Corona
6	Parra	20.49	78.48	42.4	post	1, 2	Kunhild Corona
7	Batten	15.20	217.40	65	post ?	2	Rift of Ulfrun Regio
8	Bashkirtsev	14.68	194.04	36.2	pre	6	Ghanis Chasma
9	Festa	11.48	27.25	35.3	pre ?	6	Kali Mons
10	Rhys	8.57	298.79	44	post	1	unnamed corona
11	Fossey	2.02	188.72	30.4	pre	7	Maat Mons
12	Leyster	0.96	260.04	45.8	pre	5, 6	Tenisheva Patera
13	Corpman	0.32	151.84	46	post	3	Seia Corona
14	Wen Shu	−4.48	303.68	31.5	post ?	3	Vostrukha Mons (rift associated)
15	Bascom	−10.40	302.15	34.6	pre ?	6	Khosedem Fossae rift
16	Warren	−11.72	173.53	50.9	pre	6	Dali Chasma
17	Fouquet	−15.09	203.52	47.8	post	1, 3	Unnamed rift zone
18	Winnemucca	−15.36	121.06	30.3	post	2	Kuilia Chasma
19	Jhirad	−16.85	105.58	50.3	post	2	Kuanja Chasma
20	Langtry	−16.97	154.99	50.3	post	2	Hasedom Fossae
21	Cline	−21.85	317.09	38	pre	7	Iweridd Corona
22	Isabella	−29.81	204.19	175	post	4	Nott Corona
23	Dix	−37.01	329.02	63.3	post ?	3	Innini Mons
24	Kenny	−44.35	271.05	52.7	pre	6	Abeona Mons
25	Erxleben	−50.85	39.40	31.6	post	3	Erkhe-Burkhan Corona
26	Flagstad	−54.31	18.88	39.2	post	3	Hanghepivi Chasma
27	Meitner	−55.62	321.60	149	post	3	individual flow
28	Alcott	−59.52	351.39	66	pre	6	Tarbel Patera
29	Marsh	−63.60	46.60	47.7	post	2	Okhtu-Tengai Corona

[a]Evidence of crater postdating post-regional-plains volcanics (PRPV): 1, gradual termination of crater ejecta; 2, superposition of crater outflow; 3, darkening of PRPV by crater halo; 4, darkening of PRPV by crater parabola. Evidence of crater predating PRPV; 5, sharp termination of crater ejecta; 6, obvious flood or embayment of crater and its ejecta by PRPV 7, absence of crater-related darkening of PRPV while older units are darkened.

Table 2. Dark-Parabola Craters ≥30 km in Diameter Superposed on Regional Plains and Showing Age Relations With Neighboring Post-Regional-Plains Volcanics

	Name	Latitude, deg	Longitude, deg	Diameter, km	Relation to PRPV	Evidence[a]	Source of PRPV
1	Dashkova	78.24	306.48	45.1	post	2, 4	Pomona Corona
2	Cotton	70.76	300.20	48.1	post	4	Djata Fluctus
3	Montessori	59.42	279.99	42.1	post	1, 3	60 km low Ps/Pl shield
4	Yablochkina	48.26	195.31	64.3	post	4	Razia Patera
5	Boleyn	24.41	220.05	70.4	post	4	Uzume Fluctus/Fea Fossae
6	Sitwell	16.64	190.40	32.8	post	4	Ganis Chasma
7	Adivar	8.91	76.20	30.3	post	4	unnamed fracture belt
8	Uvaysi	2.34	198.25	38.9	post/pre	1, 4/6	Ozza Mons/Maat Mons
9	Batsheba	−15.06	49.45	32.3	post	6	individual small field
10	Carson	−24.18	344.14	38.8	post	4	Menat Undae
11	Austen	−25.01	168.14	45.1	post	4	Dali Chasma
12	Boulanger	−26.63	99.25	71.5	post	4	Gefjun Corona
13	Stuart	−30.79	20.22	68.6	post	4	Vaidilute Rupes
14	Sabin	−38.51	274.73	33.1	post	4	Shivanokia Corona
15	Stowe	−43.20	233.17	80	post	4	small fields

[a]See footnote to Table 1.

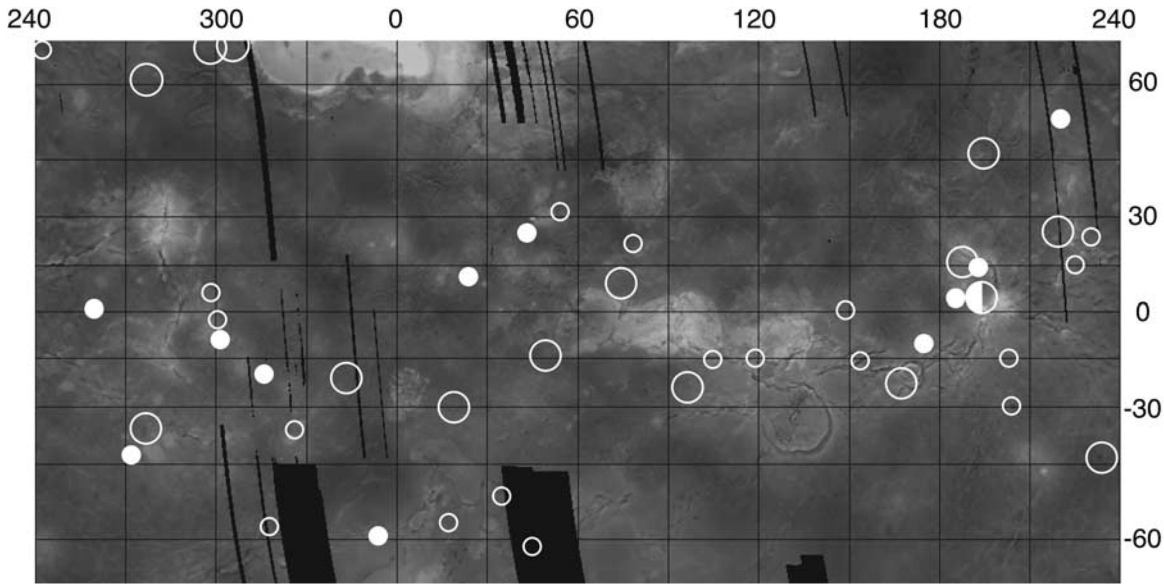

Figure 13. Craters superposed on regional plains and showing age relations with PRP volcanics on the background of the Magellan altimetry map of Venus. Larger circles are dark-parabola craters; smaller circles are nonparabola craters. Open circles designate craters postdating PRP volcanics; solid circles designate craters predating PRP volcanics.

rims should protrude through the lavas as we see, for example, in the case of the crater Gautier (see Figure 4). Thus complete burial seems to be a very rare case and probably does not cause a significant bias. The subpopulation of craters post includes craters from 30.3 to 175 km in diameter, while the subpopulation of craters pre includes craters from 30.4 to 66 km in diameter. However, if we exclude the four largest craters from the post subpopulation, it becomes very similar in size distribution to the pre subpopulation, and both of them are rather similar to the general distribution of Venus craters ≥30 km in diameter [*Schaber et al.*, 1992]. All this implies either a moderate decrease in the rate of PRP volcanism with time or, considering the relatively small numbers of the craters, a relatively constant rate of PRP volcanism.

[27] As follows from Table 2, we were able to determine the age relations with PRP volcanics for 15 dark-parabola craters. Their size distribution is rather similar to that of nonparabola craters and to the general distribution of Venusian craters ≥30 km in diameter [*Schaber et al.*, 1992]. Of these, 14 craters postdate the neighboring PRP volcanics. One crater, Uvaysi, is clearly superposed on PRP volcanics of the apron of Ozza Mons volcano (sitting at the junction of several rifts) and shows evidence that lava flows originating from Maat Mons (sitting outside of visible rifts) postdate the crater. These data show that in the time since

Table 3. Nonparabola Craters ≥30 km in Diameter Superposed on Regional Plains and Showing Age Relations With Post-Regional-Plains Rifts

	Name of Crater	Latitude, deg	Longitude, deg	Diameter, km	Relation to PRPR[a]	Name of Rift
1	Balch	29.90	282.91	40	pre	Devana Chasma
2	Romanskaya	23.22	178.44	30.4	post/pre	Ganis Chasma
3	Batten	15.20	217.40	65	post/pre	rift of Ulfrun Regio
4	Rosa Bonheur	9.73	288.78	104	post/pre	Devana Chasma
5	Higgins	8.08	241.32	40	pre	Kali Mons
6	Bascom	−10.40	302.15	34.6	pre	Khosedem Fossae rift
7	Warren	−11.72	173.53	50.9	post	Dali Chasma
8	Mowatt	−14.58	292.30	38.4	post/pre	NE of Pinga Chasma
9	Fouquet	−15.09	203.52	47.8	post	unnamed rift zone
10	Winnemucca	−15.36	121.06	30.3	post/pre	Kuilia Chasma
11	Jhirad	−16.85	105.58	50.3	post	Kuanja Chasma
12	Langtry	−16.97	154.99	50.3	post/pre	Hasedom Fossae
13	Maltby	−23.28	119.69	36.6	pre	Kuanja/Quilla Chasmata
14	Carr	−24.05	295.66	31.8	pre	Parga Chasma
15	Wiliard	−24.65	296.06	48.4	post/pre	Parga Chasma
16	Flagstad	−54.31	18.88	39.2	post	Hanghepivi Chasma

[a]PRPR, post-regional-plains rifts.

Table 4. Dark-Parabola Craters ≥30 km in Diameter Superposed on Regional Plains and Showing Age Relations With Post-Regional-Plains Rifts

	Name of Crater	Latitude, deg	Longitude, deg	Diameter, km	Relation to PRPR	Name of Rift
1	Boleyn	24.41	220.05	70.4	Post/Pre	Fea Fossae
2	Sitwell	16.64	190.40	32.8	Post	Ganis Chasma
3	Uvaysi	2.34	198.25	38.9	Post/Pre	Atla rift junction
4	Younge	−13.99	115.07	42.8	Post	East of Kuanja Chasma
5	Austen	−25.01	168.14	45.1	Post	Dali Chasma

~0.1T until the present there was no significant increase of the PRP volcanic formation rate. The postdating/predating ratio for dark-parabola craters (14.5/0.5) does not contradict the above conclusion based on observations of nonparabola craters that the rate of the PRP volcanism was slightly decreasing or close to a constant rate. If we rely on this conclusion concerning the PRP volcanism rate (slightly decreasing or constant), the 14.5/0.5 ratio is independent evidence that dark-parabola craters are indeed very young.

[28] It is interesting to analyze what types of features are related to the PRP volcanics involved in this analysis [e.g., see *Head et al.*, 1992; *Grosfils and Head*, 1996; *Stofan et al.*, 1997; *Magee and Head*, 2001]. We classified them into three categories: (1) volcanics associated with rifts (both young and old); (2) volcanics associated with coronae; and (3) others, which are volcanics associated neither with rifts nor with coronae. The volcanics of the third type are represented by rather large volcanic constructs, fields of smaller volcanic constructs, paterae, flow fields, and individual flows among older terrains. They all probably constitute a category of noncorona hot spot structures. Table 5 gives a summary of the types of PRP volcanism for 29 nonparabola craters (NPC), 18 nonparabola craters postdating the neighboring PLP volcanics (NPC-post), 11 nonparabola craters predating these volcanics (NPC-pre), and 15 dark-parabola craters (DPC) (for the latter the case of crater Uvaysi is considered as a sum of 0.5 case of rift-associated volcanics and 0.5 case of volcanics of the third type).

[29] If we compare the subpopulations of nonparabola craters postdating (NPC-post) and predating (NPC-pre) the neighboring volcanics, one can see that the percentages of the cases with rift-associated volcanics involved are not significantly different among them, and keeping in mind possible stochastic variations, we consider them as approximately the same. For the cases in which corona-associated volcanics are involved, the situation is very different: they are rather frequent among the NPC-post craters and rare among the NPC-pre craters. For the cases in which volcanics of the third type are involved, the situation is reversed: they are more frequent among the NPC-pre craters and rare among the NPC-post craters. The differences are so prominent that they are probably reliable in spite of the small numbers of craters. If the craters analyzed are distributed more or less evenly along the time axis, then volcanics formed earlier in PRP time have a better chance of being associated with NPC-post craters, while volcanics formed later in PRP time have a better chance of being

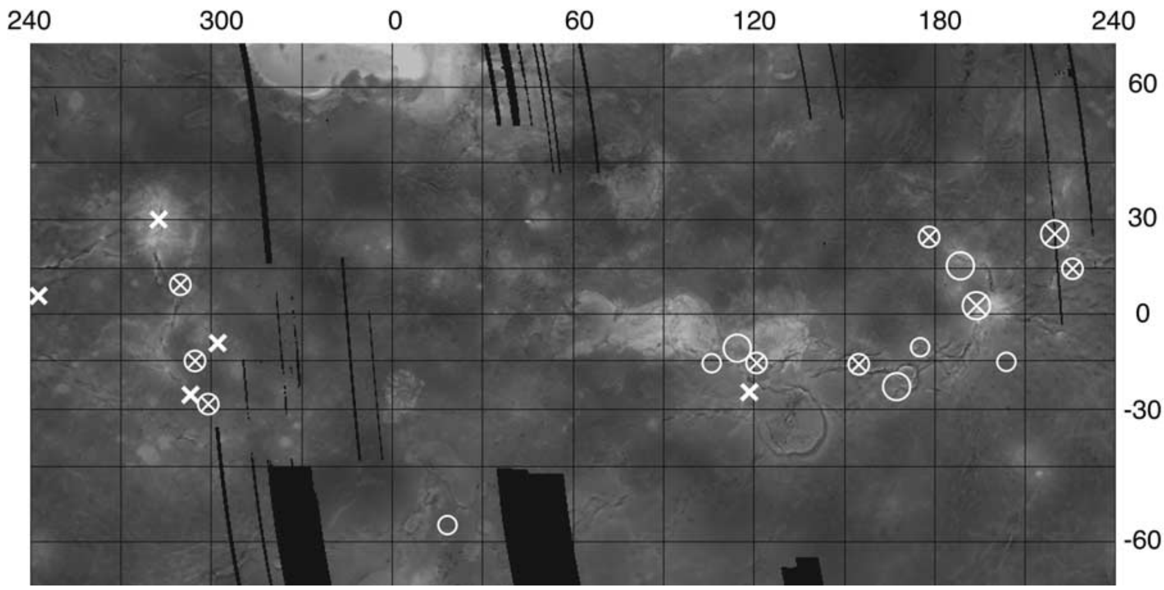

Figure 14. Craters superposed on regional plains and showing age relations with PRP rifts on the background of the Magellan altimetry map of Venus. Open circles designate craters superposed on the rifts. Crosses designate craters cut by the rifts. Crosses in circles designate craters both superposed on and cut by the rift-associated fractures. Larger symbols are dark-parabola craters; smaller symbols are nonparabola craters.

Table 5. Summary of the Types of PRP Volcanism for Nonparabola Craters, Nonparabola Craters Postdating the Neighboring PLP Volcanics, Nonparabola Craters Predating These Volcanics, and Dark-Parabola Craters

Crater Subpopulation[a]	Rift Associated		Corona Associated		Others		Total	
	Number	Percentage	Number	Percentage	Number	Percentage	Number	Percentage
NPC	10	34%	8	28%	11	38%	29	100%
NPC-post	7	39%	7	39%	4	22%	18	100%
NPC-pre	3	27%	1	9%	7	64%	11	100%
DPC	4.5	30%	3	20%	7.5	50%	15	100%

[a]NPC, nonparabola craters; NPC-post, nonparabola craters postdating the neighboring PLP volcanics; NPC-pre, nonparabola craters predating these volcanics; DPC, dark-parabola craters.

associated with NPC-pre craters. If so, one can conclude from the data in Table 5 that from the beginning of PRP time until the present, the role of rift-associated volcanism was approximately the same or slightly decreased, while the role of corona-associated volcanism decreased with time, and the role of non-corona-related volcanism of probable hot spot type proportionally increased.

[30] The general distribution of the neighboring volcanic types among the 15 cases with dark-parabola craters shows a situation resembling that observed for the total of 29 nonparabola craters: most abundant are volcanics of the third type, then follow rift-associated volcanics, and then corona-associated volcanics. It is interesting that in the only case (crater Uvaysi) when PRP volcanics are younger than the neighboring dark parabola (this implies that these lavas are really very young) these volcanics belong to the third type. This is consistent with the above conclusion that the role of volcanics of the third type increased with time.

[31] If we examine the areal distribution of craters which show age relations with neighboring volcanics (Figure 13), their nonrandom distribution is obvious, with concentration in Aphrodite, Atla, Phoebe, and Themis Regiones. This seems understandable because although the spatial distribution of craters on Venus is very close to random [*Phillips et al.*, 1992; *Schaber et al.*, 1992; *Strom et al.*, 1994; *Hauck et al.*, 1998], the spatial distribution of volcanic features (except regional plains) is certainly not random [*Head et al.*, 1992; *Crumpler et al.*, 1997; *Crumpler and Aubele*, 2000]. Thus craters selected on the basis of their spatial closeness to the PRP volcanics are expected not to be randomly distributed. If we analyze the spatial distribution of craters postdating and predating the associated volcanics, the clustering of four NPC-pre craters in Atla area is noticeable. Two of these craters (Uvaysi and Fossey) predated emplacement of lavas of the same volcano: Maat Mons. Contrary to other high mountains on Venus, this volcano lacks a radar-reflective crest that was interpreted by *Klose et al.* [1992, p. 16,366] as evidence that "Maat Mons is the youngest peak on Venus, and it may well be an active volcano." Two neighboring nonparabola craters (Bashkirtsev and Warren) predated emplacement of lavas from the young rifts [*Basilevsky and Head*, 2000b]. This may imply the presence of very recent internal activity in Atla Regio. Other craters, both predating and postdating emplacement of the neighboring PRP volcanics, do not show noticeable clustering.

[32] As is seen in Table 3, there are 16 nonparabola craters showing age relations with neighboring PRP rifts. Among them, 4 craters (25%) postdate, 5 craters (31%) predate, and 7 (44%) craters both postdate and predate rifts. This distribution agrees with the relatively constant rate of PRP rifting although because of the small number of craters, some (but not drastic) changes in the rate are not excluded. The large percentage of craters both postdating and predating rifts is evidence that rifting in many, if not in all places, when started, may have lasted for a relatively long time.

[33] As is seen in Table 4, there are five dark-parabola craters showing age relations with neighboring PRP rifts. Among them, three craters (60%) postdate and two craters (40%) both postdate and predate rifts. Because of the very small number of craters in this subpopulation, the observed age relations put no serious constraints on the rate of PRP rifting. The relatively large percentage of craters both postdating and predating rifts seems to agree with the above conclusion that rifting in many places may have lasted for a relatively long period of time. Because dark-parabola craters are believed to have formed during the last $\sim$10% of PRP time, the observation that two such craters (Boleyn and Uvaysi) are cut by part of the rift-associated fractures implies that the rifts involved (Fea Fossae and Atla rift junction) were active in geologically very recent time and may even be active at the present time.

[34] If we examine the areal distribution of craters which show age relations with neighboring rifts (Figure 14), it is obvious that they are associated with major disruption zones of Venus first described by *Schaber* [1982]. The majority of them (14 of 21) are located within the Aphrodite-Beta disruption zone, 6 craters are within the Beta-Phoebe zone, and 1 crater is within the smaller zone (55°–60°S, 320°–120°E) recently described by *Basilevsky and Head* [2000b]. Surprisingly, not a single crater $\geq$30 km in diameter showed age relations with the rift structures of the second longest Themis-Atla zone described by *Schaber* [1982]. This is probably a stochastic effect.

5. General Discussion

[35] Before we discuss the interpretation and meaning of the results of this study, we address the question of the robustness of our conclusions. The numbers we use to infer possible variations in rates and styles are rather small, so stochastic variations may play a noticeable role. If we assume that the stochastic variations in the crater subpopulations studied containing N craters follow the Poisson law, then the standard deviation $\sigma = \sqrt{N}$ [*Basaltic Volcanism Study Project (BVSP)*, 1981]. So with a high probability each N may vary within $N \pm \sqrt{N}$. The numbers which are the most crucial for our conclusions about the rates are 18 and 11 (the numbers of post and pre cases among 29 nonparabola craters showing age relations with rifts) as

Table 6. Summary of the Main Interpretations of the Numbers of Craters Postdating and Predating Neighboring PRP Volcanics and Rifts

Craters	Volcanism	Rifting
Nonparabola craters (witness time period from *T* till 0.1*T*)	relatively constant or moderately decreasing rate; relatively constant role of rift-associated volcanism, decreasing role of corona-related volcanism, increasing role of noncorona hot spot volcanism	relatively constant rate, some changes are not excluded; rather long duration of rift fracturing
Dark-parabola craters (witness time period from 0.1*T* till present)	no significant increase of the rate during the last 0.1*T*; compatible with constant or slightly decreasing rate	no constraints on the rate; confirms long duration of rift fracturing
All craters (witness time period from *T* till present)	spatial distribution follows well-known concentrations of volcanic centers (Aphrodite, Atla, Phoebe, Themis); recent activity in Atla Regio	spatial distribution follows major global disruption zones, except Themis-Atla zone (stochastic effect?); recent activity in Atla and Ulfrun Regiones

well as 4, 7, and 5 (the numbers of post, post + pre, and pre cases among 16 nonparabola craters showing age relations with craters). If we round the numbers, the expected variations are about ±3–4 cases for the craters showing age relations with PRP volcanics and are about ±2–3 cases for the craters showing age relations with PRP rifts. So changes in rates which might increase or decrease by these numbers, the observed numbers of craters in the considered subpopulations, are obviously below the accuracy of our approach. A similar procedure leads us to the conclusion of about the same order of magnitude of expected stochastic variations for the cases crucial for estimates of the roles of different volcanic types. This means that our results are rather approximate. With the data in hand we might notice changes in the rates and styles of rifting and volcanism only if they were not smaller than 30–50% of the appropriate value. It is also obvious that the considered PRP time in our considerations may be subdivided into not more than three parts: the beginning, the middle, and the end.

[36] Another issue that is important is the meaning of PRP time. Of course, by definition, it is the time since termination of formation of regional plains until the present. But if the formation of regional plains on Venus ended approximately simultaneously around the planet, this time has a meaning of a physically certain period whose duration in different areas of the planet was approximately the same. This time can be measured, for example, through the density of impact craters superposed on regional plains. If formation of regional plains on Venus ended in different areas of the planet at different times, the duration of this period in different areas was different. In this case the duration of this period of the geologic history of Venus can also be measured as the global (or regional) mean of the local durations. Which of the two models is more applicable to Venus is a subject of debate which has been underway since the early analysis of the Magellan survey of Venus [*Schaber et al.*, 1992; *Phillips et al.*, 1992; *Strom et al.*, 1994] and continues until the present [*Basilevsky and Head*, 1998, 2000a; *Guest and Stofan*, 1999; *Hansen*, 2000]. We believe that something similar to the first option is more likely to correspond to the realities of the geology of Venus. However, we do not discuss further here these alternative models because the results of our work are valid for both of these two alternatives.

[37] The results of the main interpretations of the numbers of craters postdating and predating neighboring PRP volcanics and rifts are summarized in Table 6. This summary (Table 6) shows an important result: The rates of both volcanism and rifting in the post-regional-plains time seem to be close to constant or may have some moderate variations. The observations from which these interpretations have been derived are independent of each other. At the same time, the phenomena discussed are linked in their nature: both volcanism and rifting are dependent on the thermal state of the interior of the planet, and thus the inferred conclusions concerning the rates of PRP volcanism and rifting are mutually consistent and are less likely to be the result of the stochastic play of small numbers.

[38] It was shown earlier that the mean rates of volcanism and rifting during PRP time were significantly lower than in the immediately preceding time [*Basilevsky and Head*, 1998, 2000a, 2000b]. The approximate constancy (or at least absence of noticeable variations) of the rates of PRP volcanism and rifting means, in particular, that there was no significant concentration of these activities in the beginning of PRP time. If this is so, one can infer that the change of volcanic and tectonic regimes at this time boundary (marked by emplacement of the wrinkle-ridge network) was relatively rapid. It raises the question of what geodynamic mechanism might be responsible. Keeping in mind the apparent constancy in rates, it is logical to expect that the rates of volcanism and rifting at the present time should be approximately the same as during most parts of PRP time, that is, low but not zero. The superposition of volcanics (Uvaysi) and rift-associated fractures (Uvaysi and Boleyn) on dark-parabola craters further documented in this study shows that volcanism and rifting on Venus have been active very recently and are very likely to be active at the present time.

[39] As we discussed above, the absolute duration of PRP time is approximately equal to the mean surface age of Venus, *T*. The latter is known only with large error bars. The most recent estimate by *McKinnon et al.* [1997], which generally agrees with earlier estimates of *Phillips et al.* [1992] and *Strom et al.* [1994], suggests that it is ~750 m.y. with a possible range from 300 m.y. to 1 b.y. Thus the changes (or their absence) which we inferred for PRP time were taking place on the timescale of hundreds of millions of years. This time seems to be long enough for some cooling of the planet and thickening of its lithosphere [e.g., *Brown and Grimm*, 1999]. It is not clear how significant the thickening of lithosphere could be, but it may be responsible for the inferred decrease in the role of corona-related volcanism and proportional increase in the role of non-

corona, hot spot volcanism. Geophysical modeling shows that formation and evolution of coronae seem to require a relatively thinner lithosphere [e.g., *Stofan et al.*, 1997; *Squyres et al.*, 1992; *Janes and Squyres*, 1995]. We speculate that our observations are consistent with such a model. When the lithosphere of Venus was thin enough, mantle diapirs produced the volcanic-tectonic structures of coronae. With thickening of the lithosphere, diapirs provided melt to the surface to produce the noncorona volcanic structures but were not sufficiently robust to deform the thickened lithosphere; the volcanic load of the edifices was also insufficient to cause noticeable annular lithospheric deformation.

6. Conclusions

[40] The results of this work provided the possibility of reaching conclusions concerning the potential variations in rates and styles of volcanism and rifting at the time postdating emplacement of regional plains and their deformation with the wrinkle-ridge network (PRP time; Atlian and Aurelian Periods) (Figure 1). It was found that the general rates of volcanism and rifting during PRP time were close to constant or at least had no drastic changes. At the same time these results imply a drastic change in the rates of volcanism and rifting at the boundary between PRP time and the preceding time marked by emplacement of the wrinkle-ridge network (the boundary between the Rusalkian and Atlian periods). It was also found that the role of rift-associated volcanism during PRP time was close to constant, or slightly decreasing, while the role of corona-related volcanism was noticeably decreasing, and the role of noncorona, hot spot volcanism was proportionally increasing. The latter changes may be due to thickening of the lithosphere during PRP time. The results also imply that at most if not all places where PRP rifting occurred, the rift-associated fracturing, when started, continued for a significant part of PRP time. The data show that a significant part of the PRP rifts were active in the beginning of PRP time and might be inherited from the preceding time. Our conclusions are valid both (1) for the case of a globally synchronous transition from emplacement of regional plains to the PRP regime and (2) for the case of such a transition occurring at different times in different areas of Venus.

[41] **Acknowledgments.** We thank Peter Neivert for graphic support, Anne Cote for help in manuscript preparation, Steve Pratt for computer support, and Mikhail Kreslavsky and Mikhail Ivanov for helpful discussions. This research was supported by NASA grants NAG5-4723 and NAG5-4585 to J.W.H. from the NASA Planetrary Geology and Geophysics Program and by grant "Artemida" to A.T.B. from the Russian Ministry of Science, which are gratefully acknowledged.

References

Barsukov, V. L., et al., The geology and geomorphology of the Venus surface as revealed by the radar images obtained by Venera 15 and 16, *Proc. Lunar Planet. Sci. Conf. 16th*, Part 2, *J. Geophys. Res.*, *91*, suppl., D378–D398, 1986.

Basilevsky, A. T., Age of rifting and associated volcanism in Atla Regio, Venus, *Geophys. Res. Lett.*, *20*, 883–886, 1993.

Basilevsky, A. T., and J. W. Head, Regional and global stratigraphy of Venus: A preliminary assessment and implications for the geologic history of Venus, *Planet. Space Sci.*, *43*, 1523–1553, 1995.

Basilevsky, A. T., and J. W. Head, The geologic history of Venus: A stratigraphic view, *J. Geophys. Res.*, *103*, 8531–8544, 1998.

Basilevsky, A. T., and J. W. Head, Geologic units on Venus: Evidence for their global correlation, *Planet. Space Sci.*, *48*, 75–111, 2000a.

Basilevsky, A. T., and J. W. Head, Rifts and large volcanoes on Venus: Global assessment of their age relations with regional plains, *J. Geophys. Res.*, *105*, 24,583–25,611, 2000b.

Basilevsky, A. T., J. W. Head, G. G. Schaber, and R. G. Strom, The resurfacing history of Venus, in *Venus II—Geology, Geophysics, Atmosphere, and Solar Wind Environment*, edited by S. W. Bougher, D. M. Hunten, and R. J. Phillips, pp. 1047–1086, Univ. of Ariz. Press, Tucson, 1997.

Basilevsky, A. T., J. W. Head, M. A. Ivanov, and V. P. Kryuchkov, Impact craters on geologic units of northern Venus: Implications for duration of the transition from tessera to regional plains, *Geophys. Res. Lett.*, *26*, 2593–2596, 1999.

Basaltic Volcanism Study Project (BVSP), *Basaltic Volcanism on Terrestrial Planets*, Pergamon, New York, 1981.

Brown, C. D., and R. E. Grimm, Recent tectonic and lithospheric thermal evolution of Venus, *Icarus*, *139*, 40–48, 1999.

Campbell, D. B., N. J. S. Stacy, W. I. Newman, R. E. Arvidson, E. M. Jones, G. S. Musser, A. Y. Roper, and C. Schaller, Magellan observations of extended impact crater related features on the surface of Venus, *J. Geophys. Res.*, *97*, 16,249–16,277, 1992.

Crumpler, L. S., and J. C. Aubele, Volcanism on Venus, in *Encyclopedia of Volcanoes*, edited by H. Sigurdsson, pp. 727–769, Academic, San Diego, Calif., 2000.

Crumpler, L. S., J. C. Aubele, D. A. Senske, S. T. Keddie, K. P. Magee, and J. W. Head, Volcanoes and centers of volcanism on Venus, in *Venus II—Geology, Geophysics, Atmosphere, and Solar Wind Environment*, edited by S. W. Bougher, D. M. Hunten, and R. J. Phillips, pp. 697–756, Univ. of Ariz. Press, Tucson, 1997.

Greeley, R., et al., Aeolian features on Venus: Preliminary Magellan results, *J. Geophys. Res.*, *97*, 13,319–13,345, 1992.

Grosfils, E. B., and J. W. Head, The timing of giant radiating dike swarm emplacement on Venus: Implications for resurfacing of the planet and its subsequent evolution, *J. Geophys. Res.*, *101*, 4645–4656, 1996.

Guest, J. E., and E. R. Stofan, A new view of the stratigraphic history of Venus, *Icarus*, *139*, 55–66, 1999.

Hansen, V. L., Geologic mapping of tectonic planets, *Earth Planet. Sci. Lett.*, *176*, 527–542, 2000.

Hansen, V. L., J. J. Willis, and W. B. Banerdt, Tectonic overview and synthesis, in *Venus II—Geology, Geophysics, Atmosphere, and Solar Wind Environment*, edited by S. W. Bougher, D. M. Hunten, and R. J. Phillips, pp. 797–844, Univ. of Ariz. Press, Tucson, 1997.

Hauck, S. A., II, R. J. Phillips, and M. H. Price, Crater distribution and plains resurfacing models, *J. Geophys. Res.*, *103*, 13,635–13,645, 1998.

Head, J. W., and A. T. Basilevsky, Sequence of tectonic deformation in the history of Venus: Evidence from global stratigraphic relations, *Geology*, *26*, 35–38, 1998.

Head, J. W., L. Crumpler, J. Aubele, J. Guest, and R. S. Saunders, Venus volcanism: Classification of volcanic features and structures, associations, and global distribution from Magellan data, *J. Geophys. Res.*, *97*, 13,153–13,197, 1992.

Janes, D. M., and S. W. Squyres, Viscoelastic relaxation of topographic highs on Venus to produce coronae, *J. Geophys. Res.*, *100*, 21,173–21,187, 1995.

Klose, K. B., J. A. Wood, and A. Hashimoto, Mineral equilibria and the high radar reflectivity of Venus mountaintops, *J. Geophys. Res.*, *97*, 16,353–16,369, 1992.

Magee, K. P., and J. W. Head, Large flow fields on Venus: Implications for plumes, rift associations, and resurfacing, in *Mantle Plumes: Their Identification Through Time*, edited by R. E. Ernst and K. L. Buchan, *Spec. Pap. Geol. Soc. Am.*, *352*, 81–101, 2001.

McKinnon, W. B., K. J. Zahnle, B. A. Ivanov, and H. J. Melosh, Cratering on Venus: Models and observations, in *Venus II—Geology, Geophysics, Atmosphere, and Solar Wind Environment*, edited by S. W. Bougher, D. M. Hunten, and R. J. Phillips, pp. 969–1014, Univ. of Ariz. Press, Tucson, 1997.

Namiki, N., and S. C. Solomon, Impact crater densities on volcanoes and coronae on Venus: Implications for volcanic resurfacing, *Science*, *265*, 929–933, 1994.

Phillips, R. J., R. F. Raubertas, R. E. Arvidson, I. C. Sarkar, R. R. Herrick, N. Izenberg, and R. E. Grimm, Impact craters and Venus resurfacing history, *J. Geophys. Res.*, *97*(E10), 15,923–15,948, 1992.

Price, M., and J. Suppe, Young volcanism and rifting on Venus, *Nature*, *372*, 756–759, 1994.

Price, M., and J. Suppe, Constraints on the resurfacing history of Venus from the hypsometry and distribution of volcanism, tectonism, and impact craters, *Earth Moon Planets*, *71*, 99–145, 1995.

Schaber, G. G., Venus limited extension and volcanism along zones of lithospheric weakness, *Geophys. Res. Lett.*, *9*, 499–502, 1982.

Schaber, G. G., R. G. Strom, H. J. Moore, L. A. Soderblom, R. L. Kirk, D. J. Chadwick, D. D. Dawson, L. R. Gaddis, J. M. Boyce, and J. Russell, Geology and distribution of impact craters on Venus: What are they telling us?, *J. Geophys. Res.*, *97*, 13,257–13,301, 1992.

Schaber, G. G., R. L. Kirk, and R. G. Strom, Data base of impact craters on Venus based on analysis of Magellan radar images and altimetry data, *U.S. Geol. Surv. Open File Rep.*, *98–104*, 1998. Available at http://www.flag.wr.usgs.gov.

Schultz, P. H., Atmospheric effects on ejecta emplacement and crater formation on Venus from Magellan, *J. Geophys. Res.*, *97*, 16,183–16,248, 1992.

Sharpton, V. L., Evidence from Magellan for unexpectedly deep complex craters on Venus, in *Large Meteorite Impacts and Planetary Evolution*, edited by B. O. Dressler, R. A. F. Grieve, and V. L. Sharpton, *Spec. Pap. Geol. Soc. Am.*, *293*, 19–27, 1994.

Solomon, S. C., et al., Venus tectonics: An overview of Magellan observations, *J. Geophys. Res.*, *97*, 13,199–13,256, 1992.

Squyres, S. W., D. M. Janes, G. Baer, D. L. Bindschadler, G. Schubert, V. I. Sharpton, and E. R. Stofan, The morphology and evolution of coronae on Venus, *J. Geophys. Res.*, *97*, 13,611–13,634, 1992.

Stofan, E. R., V. E. Hamilton, D. M. Janes, and S. E. Smrekar, Coronae on Venus: Morphology and origin, in *Venus II—Geology, Geophysics, Atmosphere, and Solar Wind Environment*, edited by S. W. Bougher, D. M. Hunten, and R. J. Phillips, pp. 931–965, Univ. of Ariz. Press, Tucson, 1997.

Strom, R. G., Parabolic features and the erosion rate on Venus, *Proc. Lunar Planet. Sci. Conf. 24th*, 1371–1372, 1993.

Strom, R. G., G. G. Schaber, and D. D. Dawson, The global resurfacing of Venus, *J. Geophys. Res.*, *99*, 10,899–10,926, 1994.

Tanaka, K. L., D. A. Senske, M. Price, and R. L. Kirk, Physiography, geomorphologic/geologic mapping and stratigraphy of Venus, in *Venus II—Geology, Geophysics, Atmosphere, and Solar Wind Environment*, edited by S. W. Bougher, D. M. Hunten, and R. J. Phillips, pp. 667–694, Univ. of Ariz. Press, Tucson, 1997.

A. T. Basilevsky, Vernadsky Institute of Geochemistry and Analytical Chemistry, Russian Academy of Sciences, 117975, Moscow, Russia. (atbas@geokhi.ru)

J. W. Head III, Department of Geological Sciences, Brown University, Providence, RI 02912, USA. (james_head_III@brown.edu)